Transactions of the Korean Society of Mechanical Engineers Vol. 6, No. 2, pp. 183~190, 1982.

<Original>

Computer Simulation of a Hydraulic Control System

Gon Khang and Kyo Il Lee**

(Received March 21, 1982)

유압제어시스템의 컴퓨터 시뮬레이션

강 곤·이 교 일

초 록

이 논문에서는 유압제어장치의 응답에 대하여 관성하중, 점성하중, 쿨롬(Coulomb)마찰 및 입력신호의 주파수가 시스템에 미치는 영향을 고찰하였고, 이에 따른 속도와 압력파형을 주로 서술하였다. 피스톤의 드리프트(drift)와 스프링하중을 제외한 대부분의 요소가 고려되었다.

추출된 방정식은 모두 무차원화 하였으며 입력 신호를 계단함수로 할 때에는 위치 피이드백(feedback)이 삽입되었다.

Nomenclature

A_p : Piston ram area
$B(\bar{B})$: Viscous friction coeff.
B_v : $C_d \cdot W \cdot \sqrt{\frac{2}{\rho}}$
C_d : Discharge coeff.
C_i : Internal leakage coeff.
$C_{oj}(j=1,2)$: External leakage coeff.
$F_c(f_c)$: Coulomb friction force (coeff.)
$F_s(f_s)$: Static friction force (coeff.)
$K(\bar{K})$: Spring constant
K_R : Position feedback gain (transducer gain)
$M(\bar{M})$: Total inertia of load
N : Describing function
$P_i(\bar{P}_i)(i=1,2)$: Chamber pressure
P_s : Supply pressure
P_R : Drain pressure
$Q_i(\bar{Q}_i)(i=1,2,3,4)$: Flow rate through each port
Q_{max} : Maximum flow rate
$t(\bar{t})$: Time
T_c : Time constant with no load $T_c=\sqrt{2}A_p/(B_v\cdot\sqrt{P_s})$
V_t : Total volume
$V_i(i=1,2)$: Chamber volume
W : Port area gradient
$Y_i(\bar{Y}_i)(i=1,2,3,4)$: Amount of underlapping
$y(\bar{y})$: Piston displacement
$Z(\bar{Z})$: Valve spool displacement
Z_{max} : Maximum spool displacement
β : Bulk modulus of oil
ρ : Density of oil
ω : input frequency rad/sec
$-$: Normalization with respect to $A_p\cdot P_s$, P_s, Z_{max}, Q_{max}, and T_c

* Hanyang Corporation
**Member, Seoul National Univ.

1. Introduction

The typical hydraulic control system consists of a prime mover, a pump, a servovalve, an actuator and load. Among these, a four-way hydraulic valve and a double acting cylinder were used as servovalve and actuator respec-

tively.

During the last score, the hydraulic servo-mechanism has been studied by many authors (1, 2) either in the open or closed loop. The former was dominantly taken into account in this analysis, because it is of much significance to find out the dynamic characteristics by means of sinusoidal analysis. Related to this, the system leads to non-linear differential equations. That's why computer simulation technique was employed in order to investigate each wave form of response.

The authors have studied the effects of various system parameters, especially Coulomb friction, on the basic open-loop performance.

2. Description of a Hydraulic System (Servovalve-Motor-Load)

In Fig.1 the schematic shape of a main stage of a servovalve is shown with underlapping Y_1, Y_2, Y_3, and Y_4.

In order to derive the response equation, we make the following assumptions for simplicity.

(1) The supply pressure of oil is constant.
(2) Any dilation of the hydraulic circuits due to the oil pressure does not occur.
(3) The transmission of pressure through the oil may be regarded as instantaneous on the time scale of the system.
(4) The flow through the valve port is proportional to the uncovered area, which implies that discharge coefficient does not change with Reynolds' Number, etc..
(5) Use is made of gauge pressure, so that P_R is zero.
(6) There occurs no cavitation, i.e. $P_1>0$, $P_2>0$.
(7) The temperantur of oil in tank is controlled and so the viscosity of oil may be considereed constant.

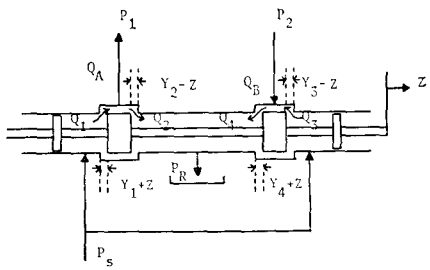

Fig. 1 Main stage of a servovalve.

Upon the above assumptions the flow rate through each port can be expressed as, by Bernoulli,

$$Q_1=\frac{1}{2}B_v[1+\mathrm{sign}(Y_1+Z)](Y_1+Z)\mathrm{sign}(P_s-P_1)\sqrt{|P_s-P_1|}$$

$$Q_2=\frac{1}{2}B_v[1+\mathrm{sign}(Y_2-Z)]\ (Y_2-Z)\sqrt{P_1}$$

$$Q_3=\frac{1}{2}B_v[1+\mathrm{sign}(Y_3-Z)]\ (Y_3-Z)\mathrm{sign}(P_s-P_2)\sqrt{|P_s-P_2|} \tag{1}$$

$$Q_4=\frac{1}{2}B_v[1+\mathrm{sign}(Y_4+Z)]\ (Y_4+Z)\ \sqrt{P_2},$$

where $B_v=C_d\cdot W\sqrt{\frac{2}{\rho}}$

and

$$\mathrm{sign}\,X=\begin{cases}+1 & \text{for } X>0\\ 0 & \text{for } X=0\\ -1 & \text{for } X<0\end{cases}$$

Y_i $(i=1, 2, 3, 4)$ is positive for open center valve, and negative for closed center valve.

The continuity equations hold between valve and actuator, so that

$$Q_A=Q_1-Q_2 \tag{2}$$
$$Q_B=Q_4-Q_3$$

If we assume (3), then equations (1) can be rewritten as (4) normalized by $Q_{\max}$.

$$Y_1=Y_2=Y_3=Y_4=Y \tag{3}$$

$$\overline{Q}_1=\frac{1}{2}[1+\mathrm{sign}(\overline{Y}+\overline{Z})]\cdot(\overline{Y}+\overline{Z})\cdot\mathrm{sign}(1-\overline{P}_1)\cdot\sqrt{2|1-\overline{P}_1|}$$

$$\overline{Q}_2=\frac{1}{2}[1+\mathrm{sign}(\overline{Y}-\overline{Z})]\cdot(\overline{Y}-\overline{Z})\cdot\sqrt{2\overline{P}_1}$$

$$\overline{Q}_3=\frac{1}{2}[1+\mathrm{sign}(\overline{Y}-\overline{Z})]\cdot(\overline{Y}-\overline{Z})\cdot\mathrm{sign}(1-\overline{P}_2)\cdot$$

$$\sqrt{2|1-\bar{P}_2|} \tag{4}$$

$$\bar{Q}_4=\frac{1}{2}[1+\mathrm{sign}(\bar{Y}+\bar{Z})]\cdot(\bar{Y}+\bar{Z})\cdot\sqrt{2\bar{P}_2}$$

$$\bar{Q}_A=\bar{Q}_1-\bar{Q}_2 \qquad \bar{Q}_B=\bar{Q}_4-\bar{Q}_3$$

where $Q_{\max}$ is the maximum flow for a critical center valve, i.e. $Q_{\max}=B_v\cdot Z_{\max}\cdot\sqrt{P_s/2}$, and the bar denotes a nondimensionalized value.

In Fig. 2 a double acting symmetrical cylinder is schematically shown as actuator.

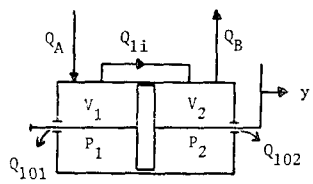

Fig. 2 Actuator.

The leakage flows can be regarded as laminar, so that their relationship with pressure is expressed in the following form.

$$Q_{1i}=C_i\cdot(P_1-P_2) \tag{5}$$

$$Q_{1oj}=C_{oj}\cdot(P_j) \qquad (j=1,2)$$

If it is assumed that the midpoint of the cyclinder is the operating point, then the continuity equation and the equation of state are combined into the normalized form.

$$\bar{Q}_A-\bar{Q}_{1i}-\bar{Q}_{1o1}=\dot{\bar{y}}+\frac{K_2+\bar{y}}{K_1}\cdot\dot{\bar{p}}_1 \tag{6}$$

$$-\bar{Q}_B+\bar{Q}_{1i}-\bar{Q}_{1o2}=-\dot{\bar{y}}+\frac{K_2-\bar{y}}{K_1}\cdot\dot{\bar{p}}_2$$

, where dot denotes differentiation with respect to the normalized time, $\bar{t}=t/T_c$, and $K_1=\beta/P_s$, $K_2=V_t/(2\cdot A_p\cdot Z_{\max})$.

From equation (6), we deduce the derivative of each pressure as computer simulation model.

Fig.3 shows a schematic load system with Coulomb friction. The pressure difference times the ram area acts as driving force F_i. The equation of motion is

$$F_i=A_p\cdot(P_1-P_2)=M\frac{d^2y}{dt^2}+B\frac{dy}{dt}+Ky+\mathrm{sign}\left(\frac{dy}{dt}\right)F_c \tag{7}$$

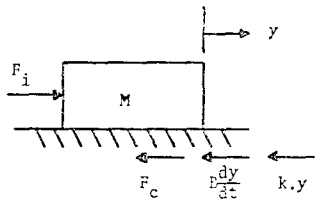

Fig. 3 Load.

Normalized by A_pP_s,

$$\bar{P}_1-\bar{P}_2=\bar{M}\ddot{\bar{y}}+\bar{B}\dot{\bar{y}}+\bar{K}\bar{y}+\mathrm{sign}(\dot{\bar{y}})\bar{F}_c \tag{8}$$

, where $\bar{M}=M\cdot Z_{\max}/(P_s\cdot A_p\cdot T_c^2)$

$\bar{B}=B\cdot Z_{\max}/(P_s\cdot A_p\cdot T_c)$

$\bar{K}=K\cdot Z_{\max}/(P_s\cdot A_p)$

$\bar{F}_c=F_c/(P_s\cdot A_p)$

are non-dimensionalized load parameters.

3. Coulomb Friction and Static Friction

Normally, friction in a servosystem would be expected to increase stability by reducing gain, but this is not always the case. Even simple servosystems sometimes exhibit low frequency limit cycle oscillations referred to as breathing, wandering, or hunting. Therefore the friction causes wear of machine tool and lowers its life.

The effect of Coulomb friction, also called dry friction, is observed as a force opposing motion of a controlled member. With the member at rest, the stiction Coulomb friction force is equal in magnitude and in opposition to the driving force. With the member in motion, the sliding Coulomb friction force is constant in magnitude, but its direction is dependent on the sense of velocity, since the force always opposes motion.

The Coulomb friction force is

$$F_c(t)=F_c\frac{\dot{y}(t)}{|\dot{y}(t)|} \qquad \text{for } \dot{y}(t)\neq 0$$

$$-F_s<F_c(t)<F_s \qquad \text{for } \dot{y}(t)=0$$

where F_s is the stiction force.

Thus the friction force F_f can be shown in Fig. 4

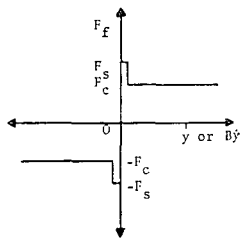

Fig. 4 Combined coulomb friction force.

4. Digital Simulation Studies

The equations derived in Chap. 2 are highly nonlinear, therefore we may well take recourse to numerical methods for solution under the assumption that no closed-form solution exists.

The integration procedure adopted here is 5-th order Runge-Kutta because it is convenient to change the step size for the accuracy of the computer program. The number of states is 4, $\overline{P}_1, \overline{P}_2$, $\bar{y}, \dot{\bar{y}}$ with the initial conditions $\overline{P}_1=\overline{P}_2=0.5$ and $\bar{y}=\dot{\bar{y}}=0$ for the first cycle.

This was programmed in FORTRAN.

In case of sinusoidal input, two hundred steps per cycle were used and the step size for step function input was 0.05 times of the time constant of corresponding system.

Table 1 Specifications.

Property	Nomenclature	Value	Programmedname
Discharge coeff.	C_d	0.61	CD
Spool diameter	D	5 mm	
Area gradient	W	15.7mm/mm	W
Density of oil	ρ	0.87kg/l	RHO
Bulk modulus	β	667,000kg/mm·s	BE
Viscosity	B	Variable	B
Spring constant	K	Variable	SC
Coulomb friction coeff.	f_c	Variable	FCOUL
Static friction coeff.	f_s	Variable	FSTAT
Supply pressure	P_s	70bar 140bar 210bar	PS

**Oil : MIL H 5606 B

It has been shown that the steady state can be reached after a few cycles in case of large inertia and sometimes after about 50 cycles when the inertia parameter becomes lower.

The most significant part of computer programming was made for the stick-slip phenomenon. The relating subroutines adopted are COMPAR, SETDT, and STICFR, which will be described later in detail.

In Table 1, the specifications used in simulation are listed.

4.1. Flow Diagram

The flow diagram is shown below.

4.2. COMPAR, STICFR

When the subject of discontinuous relations arises in regard to physical systems, the representation of such discontinuous effects on digital computer is an important part of the general subject of simulation. Therefore it may be simulated with digital equipment by using a comparator.

With methods such as Runge-Kutta, the iteration intervals may be quite large so that it is specified under consideration of accuracy. In COMPAR (subroutine), a temporary variation of the iteration interval and a search for the transition instant will be suggested.

The comparator having the velocity is deactuated whenever the absolute value of the velocity is zero; in practice, this must be interpreted as $|y|$ being less than some small but finite tolerance range, which was determined here as UTOL (10^{-5}).

The second comparator associated with stiction is actuated only when the absolute value of the driving force, $A_p \cdot \Delta P$, that is applied exceeds the stiction force F_s.

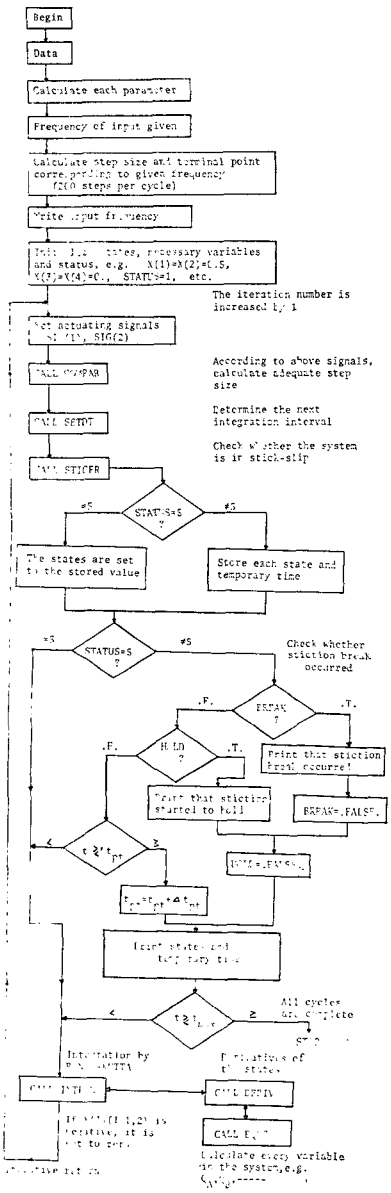

If either comparator is actuated, the forces are transmitted to the mass of the load.

5. Simulation Results

5.1. Stick-Slip

Fig.5 shows the stick-slip motion in case of sinusoidal input. As can be seen, when the velocity of the piston is reduced within the tolerance, i.e. the velocity becomes essentially zero, the piston moves no more, so far as the driving force is less than stiction force.

It is seen in Fig.6 that the stiction time increaser as the pressure difference decreases gradually.

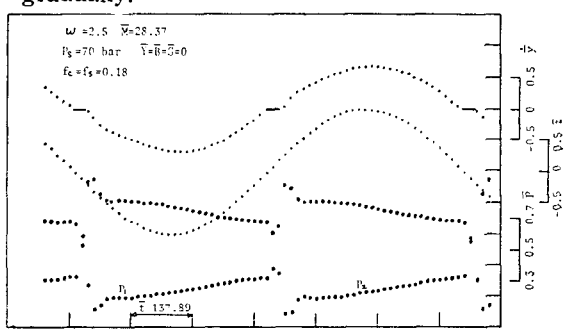

Fig. 5 Response wave with stick-slip.

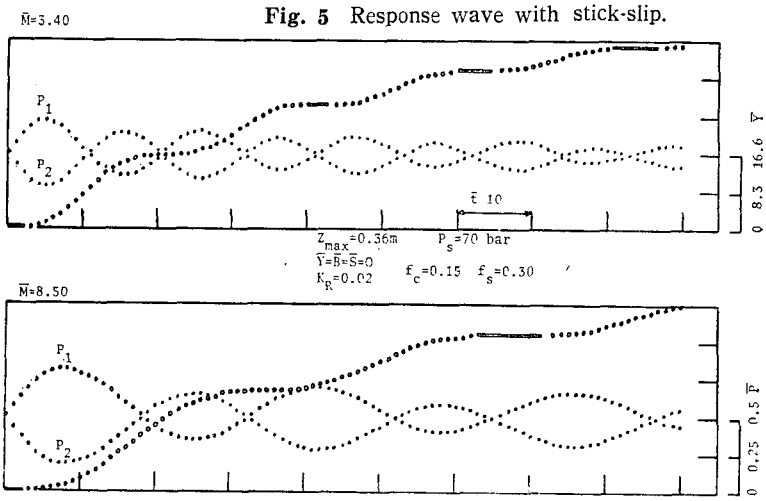

Fig. 6 Response shape with stick-slip under step input.

5.2. Effect of Load Inertia

In Fig.7 the distortion of the velocity wave

form is shown. Due to this distortion, the fundamental exhibits a phase lag. It is seen that the phase lag increases as the inertia parameter grows higher.

Montgomery and Lichtarowicz (3) have shown that at low frequencies the inertia parameter has little effect on the output amplitude.

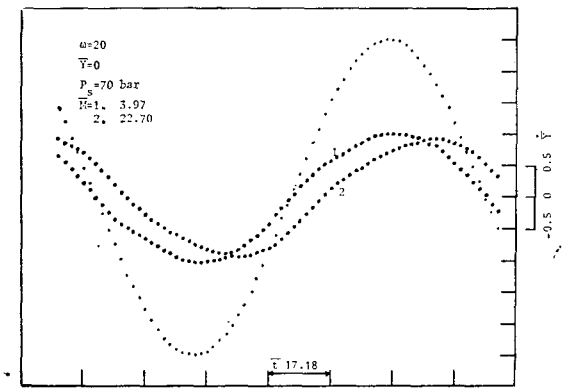

Fig. 7 Veloity with variation of inertia parameter.

5.3. Peak Pressure

A typical shape of sinusoidal response is illustrated in Fig. 8, both the simulation result and the experimental one are nearly identical except for the region where cavitation occurs (5). With digital simulation, each chamber pressure is set to zero when it decreases below zero, i.e. atmospheric pressure. It is dependent upon input frequency and load inertia when the sharp peak pressure occurs.

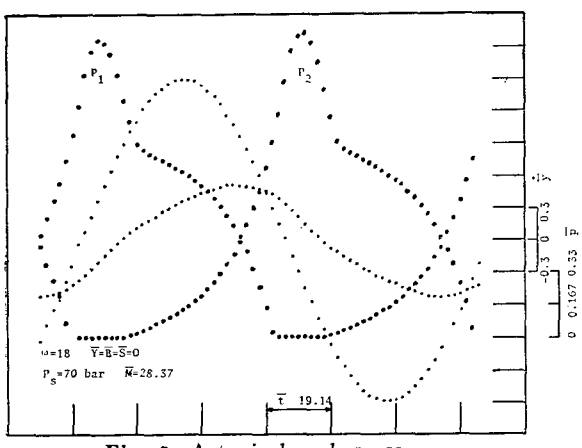

Fig. 8 A typical peak pressure.

5.4. Effect of Dashpot (Viscosity)

As illustrated in Fig. 9, although their amplitudes decrease to large extent as B increases, their phase does not alter.

For large values of viscosity parameter, their shapes tend to be rather triangular than sinusoidal. (4)

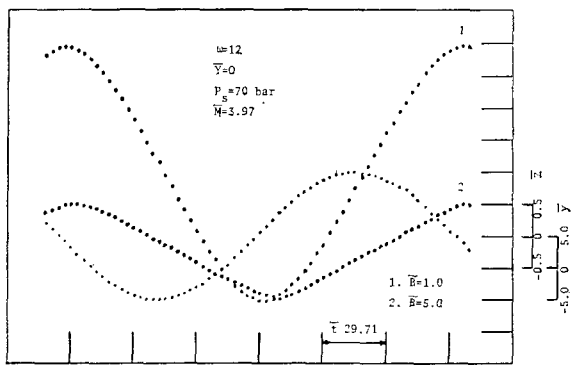

Fig. 9 Displacement with variation of viscosity.

5.5. Effect of Input Frequency

In Fig. 10, 11, 12 and 5, there are shown the response shapes of velocity and pressure under consideration of Coulomb friction, namely $f_c=f_s=0.18$, for various input frequencies. It may be stated that with low frequency each pressure changes rapidly as the valve opens or closes, and the velocity wave form shows stick-slip at that time. As the input frequency increases to some extent (Fig.11), the stick-slip can't be seen and each pressure wave becomes more sinusoidal.

When the input frequency has pretty high value, the amplitude of velocity decreases so that the piston is seen to be almost at rest and shows large phase shift of the fundamental. The velocity approaches to zero and the pressure wave becomes nearly sinusoidal when in much higher frequency.

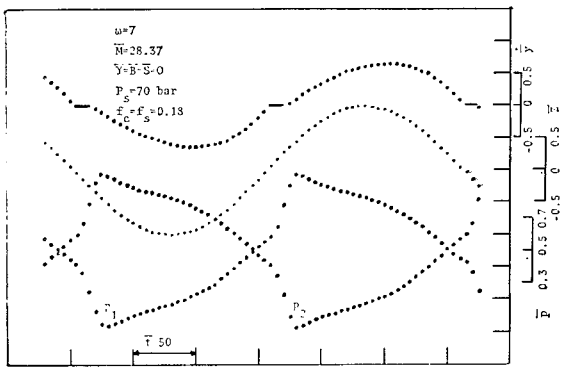

Fig. 10 Response wave with variation of frequency.

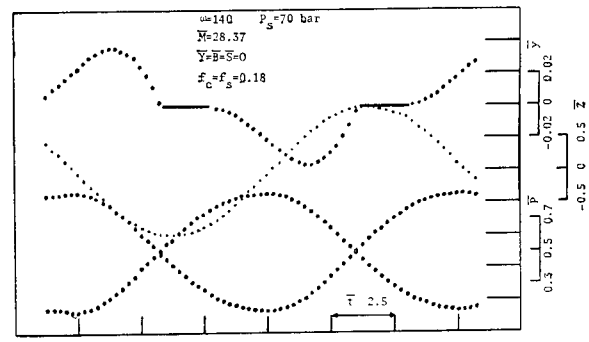

Fig. 12 Response wave with variation of frequency.

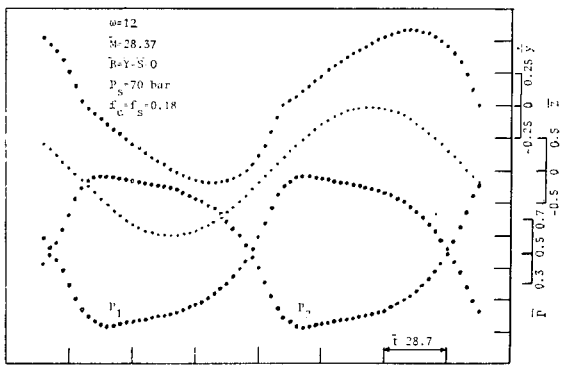

Fig. 11 Response wave with variation of frequency.

5.6. Response of step Function Input

The stick-slip phenomena also depend on the system parameters under step function input Their effects are shown in Fig. 6, 13, and 14.

6. Conclusion

The response of a hydraulic control system including stick-slip phenomena have been

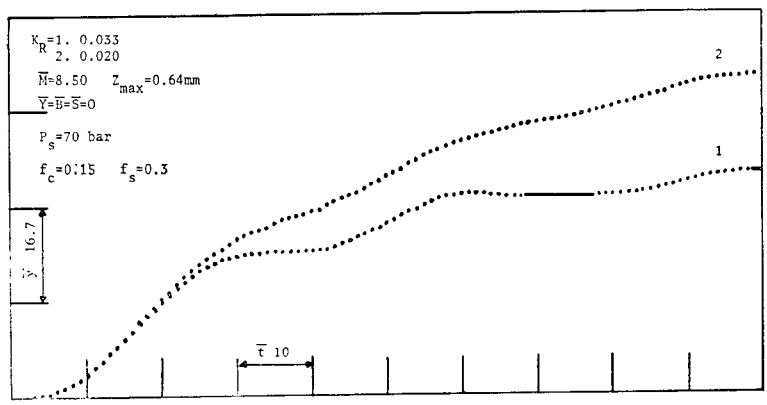

Fig. 13 Response shape with stick-slip for different feedback constant.

obtained through computer simulation and these may be used to predict the performance of the system as following.

(1) High inertia papameter increases the peak pressure in the actuator and the phase lag of velocity of the fundamental and reduces the amplitude of oscillation of the ram.

(2) Underlap decreases the peak pressure a little compared with the other lap conditions, and they show different wave shapes in pressure.

(3) The displacement form becomes more triangular and smaller in amplitude with the increase of viscosity.

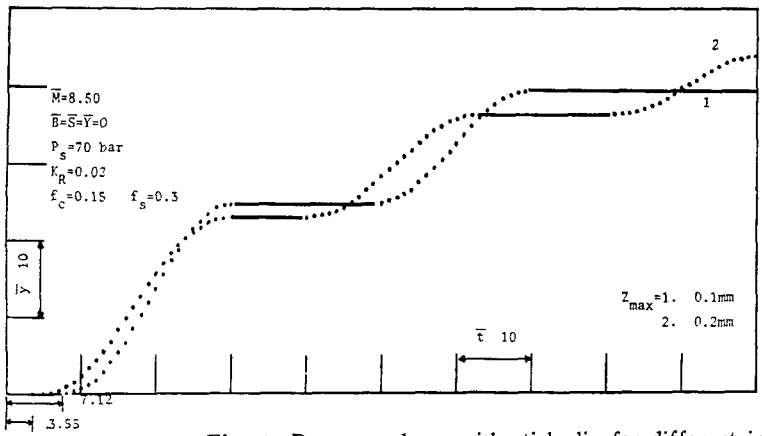

Fig. 14 Response shape with stick-slip for different input magnitude.

(4) At low frequency, the stick-slip motion is observed. In case of very high frequency, the pressure wave becomes nearly sinusoical and the velocity shape vanishes.

(5) In case of step function input, the stick-slip becomes dominant with the decrease of feedback constant and input magnitude or when with high inertia parameter.

(6) Dither signal superposed upon input shows less effect under sinusoidal input than under step one.

References

1. D. McCloy and H.R. Martin, Control of Fluid Power. Ellis Horwood, 1980.
2. T.J. Viersma, Analysis, Synthesis and Design of Hydraulic Servosystems and Pipelines, Elsevier, 1980.
3. J. Montgomery and A. Lichtarowicz, Asymmetrical Lap and other Nonlinearities in Valve-Controlled Hydraulic Actuators, Proc. of the Mech. Engineers, Vol. 183, pt. 1, No. 40, pp.663-683, 1968-69.
4. D.E. Turnbull, The Response of a Loaded Hydraulic Servomechanism, Proc. of the Mech. Engineers, Vol. 173, No. 9, pp.270-284, 1959.
5. K.I. Lee, Dynamisches Verhalten der Steuerkette Servoventil-Motor-Last, Diss. TH Aachen, 1977.